

# Sigmoids as Precursors of Solar Eruptions

Richard C. Canfield, Hugh S. Hudson, Alexei A. Pevtsov

*Abstract*—Coronal Mass Ejections (CMEs) appear to originate preferentially in regions of the Sun’s corona that are sigmoidal, i.e. have sinuous S or reverse-S shapes. *Yohkoh* solar X-ray images have been studied before and after a modest number of Earth-directed (halo) CMEs. These images tend to show sigmoidal shapes before the eruptions and arcades, cusps, and transient coronal holes after. Using such structures as proxies, it has been shown that there is a relationship between sigmoidal shape and tendency to erupt. Regions in the Sun’s corona appear sigmoidal because their magnetic fields are twisted. Some of this twist may originate deep inside the Sun. However, it is significantly modulated by the Coriolis force and turbulent convection as this flux buoys up through the Sun’s convection zone. As the result of these phenomena, and perhaps subsequent magnetic reconnection, magnetic flux ropes form. These flux ropes manifest themselves as sigmoids in the corona. Although there are fundamental reasons to expect such flux ropes to be unstable, the physics is not as simple as might first appear, and there exist various explanations for instability. Many gaps need to be filled in before the relationship between sigmoids and CMEs is well enough understood to be a useful predictive tool.

*Keywords*—Sun, magnetic fields, coronal mass ejections

## I. INTRODUCTION

The launch of *Yohkoh* in 1991 greatly extended our capability for making direct X-ray images of the hot solar corona, in the natural emission domain characterized by photon energy  $h\nu \sim kT$  from a million-degree gas. Prior to *Yohkoh*, the Skylab mission and several sounding rockets had carried soft X-ray telescopes for solar observation. The *Yohkoh* SXT [1], [2] observations offered improved temporal cadence and span,  $\sim 100$  full disk images per day from late 1991 to the present. The movie representation of these data in particular has been eye-opening.

As viewed in X-rays, coronal active regions consist of discrete bright loops that outline magnetic field lines. These loops (Fig. 1) often collectively form sinuous S or inverse-S shapes [2] termed *sigmoids* by Rust and Kumar [3]. They found transient X-ray brightenings that typically evolved from bright, sharp-edged sigmoidal features into either an arcade of loops or a diffuse cloud. The latter phenomena – part of long-duration events, or LDEs – were discovered in the Skylab era of X-ray imaging [4], [5], [6].

The concept of *magnetic helicity* [7], which has been explored in laboratory and space plasmas to a substantial extent, provides a useful framework with which to characterize twisted magnetic fields on the Sun. We know that the overall twist of active region magnetic fields, as observed both at the visible surface of the Sun (photosphere)

and corona are related [8]. We expect transient sigmoidal brightenings to form within regions whose overall magnetic structure is twisted. Moreover, we know that the large-scale twist of active regions seen in the photosphere changes little from day to day [8]. Hence, there is reason to expect active regions whose large-scale, long-lived structure is sigmoidal to be associated with eruptive phenomena.

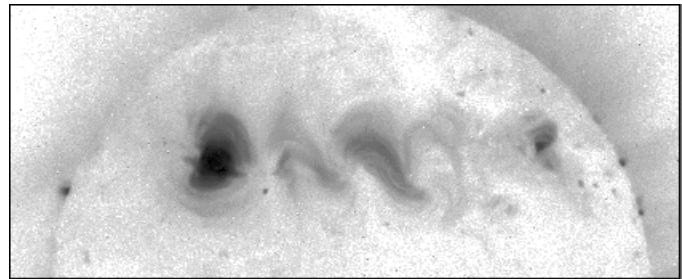


Fig. 1. *Negative* images of coronal X-ray loops seen in the northern hemisphere by the *Yohkoh* SXT. The region near the central meridian, and the fainter one immediately to its left, show the inverse-S pattern of loops that is more common in the Sun’s northern hemisphere. The much brighter region still farther to the left is a simple bipolar region with no hint of sigmoidal structure.

In this paper we concentrate on observations of sigmoids in X-rays made with the *Yohkoh* SXT (Sec. II) and related observational studies of twisted magnetic fields in the underlying photosphere (Sec. III), theoretical studies of the origin, stability, and eruption of magnetic fields (Sec. IV), and topics for future research (Sec. V). For a comprehensive review of other phenomena associated with coronal mass ejections we refer the reader to Webb’s paper in this issue [6].

## II. CORONAL AND SOFT X-RAY OBSERVATIONS

The SXT observations show the corona as a function of time, and coronal mass ejections come from the same corona, so it would seem reasonable to have expected the immediate discovery – soon after the *Yohkoh* launch in 1991 – of the mechanisms of CME formation. However, classical CME observations come from optical telescopes (coronagraphs) which can observe the corona only above the limb of the Sun. The SXT could detect a CME-launching disturbance anywhere on the disk, in principle, though emission in X-rays ( $\sim n_e^2$ ) falls off with height in the corona much more rapidly than emission in the optical region ( $\sim n_e$ ). For these and other reasons, the main CME signatures were understood only several years after *Yohkoh* was launched. The key advance in instrumentation has been the large field of view and high sensitivity of the LASCO coronagraphs [9] on the SOHO mission, combined with the high-temperature sensitivity ( $\sim 3MK$ ) of the *Yohkoh* SXT.

R. Canfield and A. Pevtsov are at the Department of Physics, Montana State University, Bozeman. E-mail: canfield@physics.montana.edu, pevtsov@physics.montana.edu

H. Hudson is with the Solar Physics Research Corporation, Institute of Space and Astronautical Sciences (ISAS), Sagamihara, Japan. E-mail: hudson@isass1.solar.isas.ac.jp.

These earlier data had shown clearly that X-ray arcades – ideally, long nearly-cylindrical rows of magnetic loops containing heated plasma – formed in the solar corona at the times of CME launches. Moreover, the arcades frequently appeared to grow out of coronal magnetic structures exhibiting *shear*, observationally defined as the tendency of coronal loops to lie obliquely across the magnetic polarity inversion line in the photosphere beneath them. The arcade formation thus appeared to be a relaxation of this shear to a more nearly perpendicular loop system. This realization spawned much theoretical work, mostly in the ideal MHD approximation, regarding structural stability and especially the consequences of magnetic reconnection. Theoretical work continues vigorously, as summarized below, paying particular attention to the structure of sigmoids.

#### A. CMEs and Halo CMEs

The LASCO coronagraphs (observations beginning in 1996) quickly offered an opportunity to calibrate the X-ray signatures being discovered with *Yohkoh*, and the EUV instrumentation on board SOHO added further new perspectives (see below). In particular LASCO surprised us [10] by detecting many more “halo CMEs” at a much greater rate than had been found with earlier coronagraphs (notably the ones on the Skylab, SMM, and P78-1 spacecraft). A halo CME is one that extends all or most of the way around the occulting edge of the coronagraph [11]. From the geometry one infers that the cloud of gas must lie along the Sun-Earth line, moving either away from or toward the Earth, and in the latter case an impact with Earth is likely.

The greater rate of halo CMEs, resulting mainly from the superior performance of the LASCO coronagraphs, provides us with a double reward: first, there is the obvious advantage in forecasting terrestrial effects, since the halo events may come straight at Earth and have high “geoeffectiveness.” Second, these events occur near disk center, ideal for the X-ray, EUV, and other observations to learn about the physics of the eruption process.

Another LASCO surprise came in a new understanding of the so-called “disconnection events.” Cartoons of the standard two-dimensional picture of magnetic reconnection showed the pinching-off of magnetic field lines below the CME, with the underlying reconnected field lines forming an arcade. This picture predicts the occurrence of concave-outward magnetic structures in coronagraph images of CMEs, but the most thorough studies [12] failed to find many cases. LASCO has found many more, but the bulk of them appear to result from the outward motion of large-scale helical structures, *flux ropes*, rather than pinching-off (but see the excellent example of the latter presented by [13]).

#### B. X-ray signatures

It has been known for some time that arcade formation is an X-ray signature of a CME [4], [14], [6]. For some time we have also known of the association of “transient coronal holes” with eruptive flares (e.g., [15]). Because true coronal

holes had been identified as the sources of high-speed solar-wind streams already, the presence of sudden darkening near arcade flares suggested the transient opening of strong active-region fields at the sites of CME launches.

The *Yohkoh* observations allowed us to generalize the observation of transient coronal holes, with a collection of phenomena termed “dimming” [16], as illustrated in Figure 2. This name has a neutral connotation relative to interesting and as-yet-unsolved questions regarding the manner of opening and closing magnetic field lines (here “opening” means the ejection of magnetized plasma far enough from the solar surface to participate in the solar-wind flow). Table I lists the categories of dimming events now known to occur in coronal X-ray imaging [17], [18].

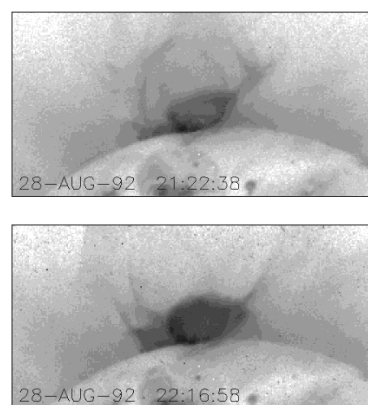


Fig. 2. Two soft X-ray images from *Yohkoh*, demonstrating the dimming of the corona above an arcade flare event seen side-on. The filamentary structures seen in the upper image (earlier) fly away from the flare, leaving a void. We interpret such a dimming as the result of mass loss into the solar wind, following the opening of the magnetic field lines immediately surrounding the arcade [17]. Unfortunately at the time of this event (August 28, 1992) we had no access to coronagraph data.

TABLE I  
X-RAY TRANSIENT DIMMINGS

| Dimming type            | Reference |
|-------------------------|-----------|
| Transient coronal holes | [15]      |
| Enveloping dimming      | [16]      |
| Arcade dimming          | [19]      |
| Moving cloud            | [20]      |
| Transequatorial loop    | [18]      |

The different categories refer to the morphology of the dimming structure. Dimming in general has its easiest interpretation in terms of the expulsion of mass from the corona, hence a CME; in the best of cases (“moving cloud”) one can also actually see the motion of the material, but the high-temperature plasma visible in soft X-rays often has such a diffuse character that the flow cannot easily be recognized.

### C. EUV signatures

The EUV Imaging Telescope (EIT) on SOHO brought still further perspectives on mass ejections from the lower corona. We had known about large-scale coronal shock waves from the early meter-wave observations of Type II bursts (e.g. [21]); rapidly-expanding wave-like fronts also could be seen as “Moreton waves” via H $\alpha$  observations of the chromosphere [22] – the latter seemed mysterious because their speeds exceeded theoretical limits. Uchida [23] united these observations with the interpretation that a rapidly-expanding global coronal wave would focus energy into its chromospheric skirt, so that the Type II burst and Moreton wave could represent two different views of weak fast-mode Alfvénic disturbances launched by a flare into the corona.

This simplification (a flare-driven blast wave) did not lead easily to an explanation for shocks seen in the outer corona and solar wind. Here the CME itself, not the effects of the flare eruption directly, drives a *different* shock wave (e.g. [24]). Thus many events with powerful flares and CMEs apparently create two distinct large-scale coronal waves. At present we cannot readily identify these separate signatures in coronagraphs, but the halo CMEs [11], [10] may eventually provide a link.

With *Yohkoh*’s new X-ray view of the solar corona, commencing in 1991, one might confidently have expected to see the Type II/Moreton shock fronts more directly. In fact this did not happen until the EIT instrument on SOHO began routine high-cadence observations in 1997 [25]. These observations have shown the common occurrence of these large-scale waves, frequently in association with halo CMEs. Although the soft X-ray observations frequently show ejecta from flares, signatures resembling the EIT waves have not been found readily (see [26] for a discussion of the implications of this, along with a description of a plausible X-ray signature from a flare of May 6, 1998).

### D. The “sigmoid $\rightarrow$ arcade” signature

The recognition that coronal structures change from a sheared (apparently twisted) to a less-sheared magnetic configuration during major eruptive flares (e.g. [4], [27]) led to much of the theoretical development described below. The *Yohkoh* soft X-ray observations gave us the new finding that the pre-event magnetic shear often takes the form of a sigmoidal coronal structure at an elevated temperature.

The sigmoid may suddenly disappear (or become modified) during a CME launch [28], [29], [30], in the pattern that we term the “sigmoid  $\rightarrow$  arcade” signature (Figure 3). Transient coronal holes – one of the dimming signatures indicating a CME occurrence – often form in the crooks of the sigmoid. This pattern occurred repeatedly in a study of low-coronal counterparts of halo CMEs [30].

The possible utility of this phenomenology is clear: we may use it to assist in predicting the occurrence of CMEs, which may have hazardous effects at the Earth. How good is this new tool? A first survey of the statistics of this

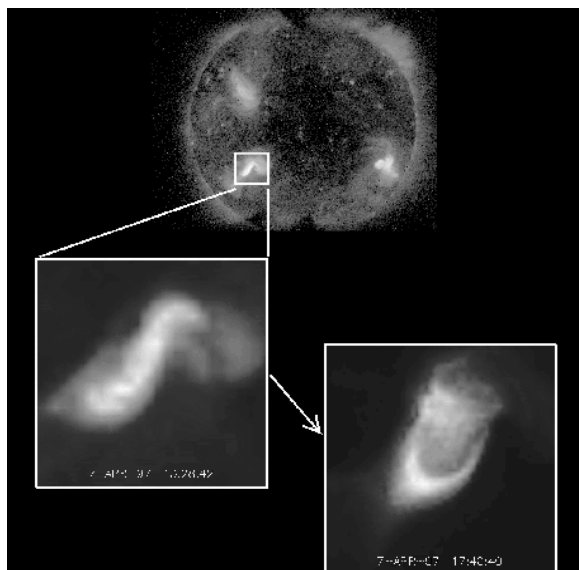


Fig. 3. Illustration of the “sigmoid  $\rightarrow$  arcade” morphology, in which a sigmoidal coronal structure (left insert, 7-APR-97 13:28:42 UT) erupts, leaving behind an arcade and a cusp (right insert, 7-APR-97 17:40:40). From A. Sterling, by permission.

question [31] examined two descriptors of solar active regions: the sunspot area and the tendency towards helicity. The latter consisted of a simple shape classification into “sigmoid” or “non-sigmoid.” These descriptors were then compared with occurrence of eruptions, using the X-ray morphology (cusps, arcades, directly observable ejections, dimmings). Both descriptors correlated positively with the tendency towards eruption (Figure 4). The results quantitatively confirm the finding of Rust and Kumar [28] regarding the association of sigmoids and eruptions. The association between sunspot area and probability of eruption has long been known [32].

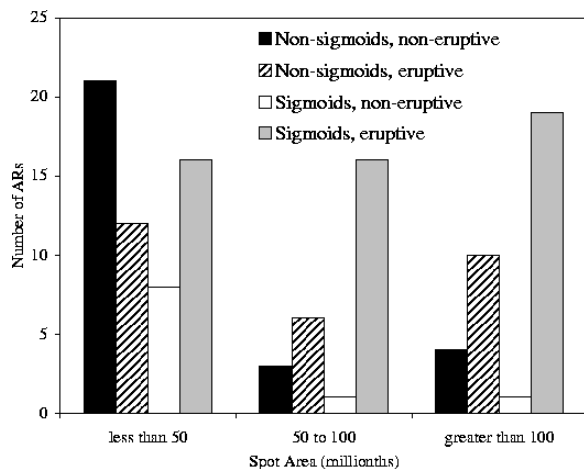


Fig. 4. Statistics relating the appearance of sigmoid morphology and of active-region size to eruptions [31].

### III. MAGNETIC FIELD OBSERVATIONS

#### A. Solar active regions

Magnetic fields play an important role in all active phenomenon on the Sun, including CMEs. Due to the highly ionized state of the solar corona, magnetic field is “frozen” into the plasma. At and below the photosphere, the magnetic field topology may be changed by plasma motions. Above the photosphere, however, the plasma must follow existing magnetic field lines.

Magnetic flux is thought to be generated by a dynamo operating at the base of the solar convection zone, approximately 200,000 km below the photosphere. In the dynamo region, magnetic fields are organized in individual flux tubes. When the field strength in a flux tube exceeds a threshold, it becomes buoyant and rises to the photosphere, where it forms a solar active region with magnetic regions of conjugate polarity. Thus, the active region can be pictured as the upper part of a large  $\Omega$ -shaped loop, whose apex is in the corona, above the photosphere, and whose legs are anchored at the base of the convection zone.

#### B. Constant $\alpha$ force-free field

Above the photosphere, magnetic forces become dominant over those of gravity and gradients of the gas pressure. Electric currents flow along magnetic field lines, and the field is described by the force-free field model  $\nabla \times \mathbf{B} = \alpha \mathbf{B}$ , where  $\mathbf{B}$  is the magnetic induction [33]. Solar magnetographs use the polarization of spectral lines to measure the magnetic field vector in the photosphere, but these techniques do not work in the corona. However, the coronal magnetic field can be modeled in various ways; one of the simplest is to use the linear force-free field approximation with  $\alpha = \text{constant}$ , using a photospheric vector magnetogram as a boundary condition. If this is done in a simple bipolar active region, and the field lines are projected onto the horizontal plane, the extrapolated field lines form a distinctive sigmoidal pattern (Figure 5, left panel) reminiscent of the letter S (for  $\alpha > 0$ ) or a backwards S ( $\alpha < 0$ ). Sigmoidal structures are not unusual in the solar corona (Figure 5, right panel).

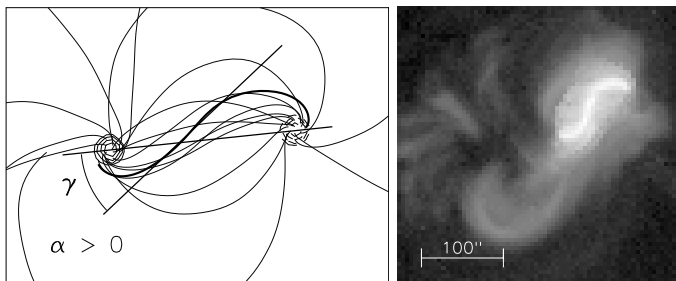


Fig. 5. Model linear force-free field for a simple bipolar region with positive  $\alpha$  (left) and Yohkoh SXT image showing an S-shaped sigmoidal structure (right).

#### C. Relation of coronal twist to the photosphere

The close similarity in appearance between the shapes of force-free field lines and those of coronal structures (Figure

5) supports the use of this model. Using photospheric magnetograms, one can compute linear force-free fields with various values of  $\alpha$ . The “best” value of  $\alpha$  then can be determined by minimizing the difference between the computed and observed patterns of fields in a least-squares sense [34]. Coronal  $\alpha$  values can be determined independently as  $\alpha = \frac{\pi}{d} \cdot \sin \gamma$ , where  $d$  is the separation between footpoints of a loop and  $\gamma$  is the shear angle (Figure 5). There is a good correlation between the photospheric and coronal values of  $\alpha$ , which suggests a continuity of electric currents flowing through the photosphere and corona above an active region [8]. At least two different processes can contribute to photospheric electric currents and corresponding shear in the coronal loops: gradual build-up by steady near-surface motions [35], and sub-photospheric motions unrelated to those visible in the photosphere [36].

TABLE II  
CHIRALITY OF SOLAR ACTIVE REGIONS [37] AND SHAPE OF THE CORONAL SIGMOIDS [38] BY HEMISPHERE.

|                   | N-hemisphere | S-hemisphere |
|-------------------|--------------|--------------|
| Positive $\alpha$ | 38%          | 66%          |
| Forward S         | 41%          | 68%          |
| Negative $\alpha$ | 62%          | 34%          |
| Backward S        | 59%          | 32%          |

#### D. Hemispheric chirality rule

The distribution of the chirality (handedness) of active region magnetic fields follows a weak hemispheric rule. The chirality of a given active region may be determined from either the  $\alpha$ -coefficient based on a photospheric magnetogram or the shape (S or backwards-S) of the coronal loops. Approximately 60-70% of active regions in each hemisphere exhibit a preferred chirality, as detailed in Table II. The chirality of active regions in the photosphere tends to be negative in the northern hemisphere, and positive in the southern. Coronal loops tend to show S shapes in the southern hemisphere (easy to remember); we see below that this is consistent with the observed photospheric chirality [38].

The interaction between magnetic fields and both turbulent convection-zone plasmas (whose kinetic helicity depends on hemisphere) and differential solar rotation (whose direction of shear depends on hemisphere) are likely sources of the hemispheric chirality rule [39], [35].

We expect the hemispheric chirality rule and the solar magnetic cycle to come into play in the reconnection of geomagnetic fields with those of solar eruptions. The mutual orientation of these two fields affects the reconnection rate and hence the geoeffectiveness of the CMEs [40].

#### E. Helicity and stability

In Sec. III-D we identified two processes which may contribute to the formation of twisted magnetic fields. A sigmoid of given length may be formed by reconnection of two

smaller loops. The total amount of twist in a given loop is a factor in its MHD stability [33]. A simple model illustrates this point. Consider a cylindrical force-free magnetic field with constant  $\alpha = T/L$ , where  $L$  is the length of the tube and  $T$  is the total twist contained within it. The tube is stable to the MHD kink instability for total twist below a critical value  $T_c \sim 2\pi$ . Reconnecting two stable flux tubes can result in a total twist  $T_1 + T_2 > T_c$ . Figure 6 gives an observation associated with an eruption [41] that appears to conform to the above scenario.



Fig. 6. Sequence of *Yohkoh* soft X-ray images showing the formation of a sigmoidal structure before the eruptive flare of 1992 May 8 15:12 UT, which took place between two last panels. The arrow shows the gap between two individual flux tubes at an early stage of the event.

The interplanetary magnetic field exhibits flux-rope properties in many CMEs, perhaps most of them. Estimates of the fraction that do so range from 1/3 [42] to nearly all [43]. Figure 7 shows how, as the result of several reconnection events, the magnetic field might become disconnected from the solar surface and erupt. Multiple reconnection events leading to the buildup of larger-scale twisted flux ropes and subsequent eruption have been found in one well-observed event [44].

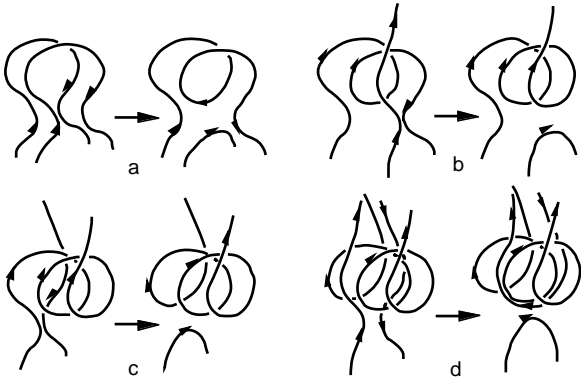


Fig. 7. The sequence of the reconnection events in the corona leading to disconnection of the magnetic field from the solar surface and formation of a CME. By permission [42]

#### F. Helicity and reconnection

It appears that helicity comes into the reconnection process in two ways, which are illustrated by contrasting reconnecting twisted fields in the laboratory and the Sun. Consider the drawing in Figure 8a, which illustrates reconnection of twisted cylinders in two cases, whose chirality is the same (left column) or opposite (right column).

Laboratory plasma experiments show that the rate at which magnetic reconnection takes place between two flux

systems is greater when their chirality is opposite (counter-helicity) [45]. In the laboratory (Figure 8b), reconnection is favored when field lines at the interface between two reconnecting twisted field systems are fully anti-parallel (right column).

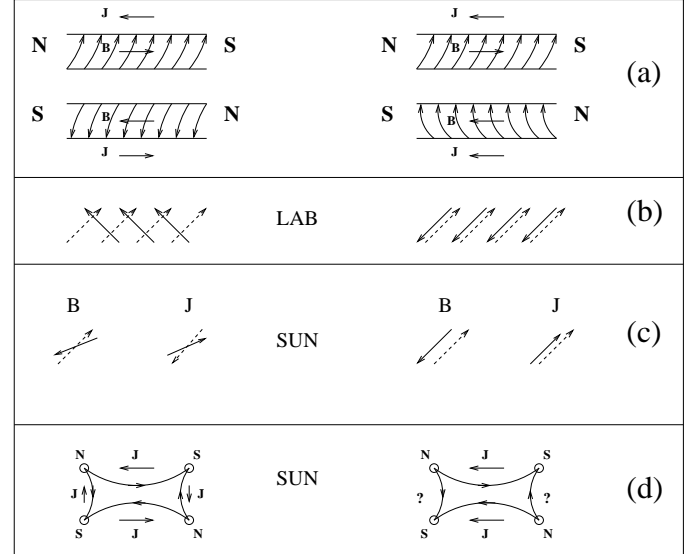


Fig. 8. Two scenarios of reconnection between two twisted flux tubes having (left) same and (right) opposite chirality. (a) Schematic representation of pair of flux tubes. Arrows show the longitudinal components of the field and electric currents. Orientation of the field and electric currents in the reconnection site in (b) plasma laboratory experiments and (c) on the Sun. (d) topology of the magnetic field and currents in the post-reconnection complex, viewed from above.

The solar corona, however, seems to favor reconnection when the chirality is the same (co-helicity) [46]. The difference from the laboratory result can be attributed to the lesser pitch of the twisted solar magnetic fields, which have much more nearly the same orientation at the reconnection site, independent of chirality (Figure 8c). The solar result has been attributed to the role of the field-aligned electric currents associated with the twisted fields. The direction of currents relative to magnetic field is chirality-dependent. On the Sun, the counter-helicity reconnection must dissipate significant currents, and hence is less favorable from the point of view of continuity [46] (cf, Figure 8d left and right) and energetics [47].

The existence of transequatorial interconnecting loops [48], [49], [50], [51] implies to us that large-scale magnetic reconnection has taken place, since we know of no way that either the solar dynamo or sub-photospheric magnetic flux propagation will create them. Table III shows statistics for transequatorial loops connecting 27 pairs of close active regions. In most cases transequatorial loops between two such regions develop only if they have the same chirality. In contrast, interconnecting loops do not tend to develop between regions of opposite chirality, despite their proximity.

TABLE III  
TRANS-EQUATORIAL CONNECTIONS AND CONJUGATE-REGION  
CHIRALITY FOR 27 PAIRS OF ACTIVE REGIONS.

| Connected ? | Opposite | Same |
|-------------|----------|------|
| Yes         | 2        | 15   |
| No          | 8        | 2    |

### G. Nests of activity and helicity.

Several studies show that active regions tend to form repeatedly in certain areas, called nests of activity, which may last for up to six months (6 solar rotations). Observations suggest a spatial relationship between the origin of CMEs and the nests of activity [52]. Large-scale helicity patterns, perhaps related to nests of activity, have also been found [53], [54]. Active regions that disobey the hemispheric helicity rule tend to emerge at certain locations, which could be called nests of helicity, in analogy to nests of activity. Bearing in mind the importance of twist to reconnection (Sec. III-F) and MHD stability (Sec. III-E), one should expect to find a statistically higher probability of eruptions near activity and helicity nests.

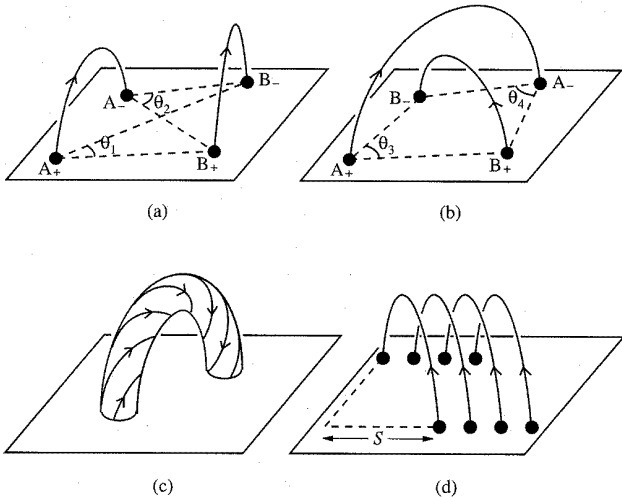


Fig. 9. Building blocks of coronal magnetic fields: (a) nearby flux tubes; (b) crossing flux tubes; (c) a twisted flux tube; (d) a sheared arcade. The black dots mark the photospheric footpoints of the coronal field lines. By permission [55].

## IV. THEORY

Theoretical studies have focused on several basic issues:

- How are flux ropes formed?
- How are sigmoids related to flux ropes?
- Why do sigmoids erupt?

In all probability, twisted magnetic fields are created deep inside the Sun [57], [39]. In the corona, such magnetic helicity [7] manifests itself in several forms (Fig. 9). Sigmoidal structures, whose sinuous structure suggests non-zero helicity, have been explained in several ways. It ap-

pears to us that no single formation mechanism accounts for sigmoidal structures seen on the Sun; whereas the emergence of twisted flux tubes (Fig. 9(c)) may be a plausible explanation of sigmoids in active regions, those seen outside active regions may best be explained in terms of shearing by differential rotation and diffusion.

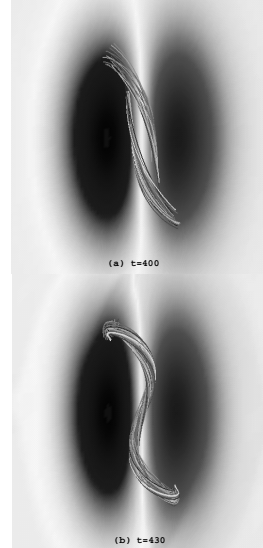


Fig. 10. Merging of magnetic field lines in a 3D nonlinear MHD simulation, as the previously twisted and sheared configuration adjusts to the emergence of opposite-polarity magnetic flux. Time is in units of the Alfvén time. By permission [61].

### A. Formation of twisted magnetic fields

On scales much smaller than observed sigmoids, twisted flux such as that drawn in Fig. 9(c) is observed to emerge from beneath the solar photosphere [36]. The much larger structures seen as sigmoids in the corona and flux ropes in the interplanetary medium may result from reconnection of smaller ones. Helical field lines may form by reconnection after magnetic flux has emerged into the corona, in either twisted or untwisted form [35], [42]. Random footpoint motion, modeling the effect of photospheric supergranular motions, combined with shearing footpoint motion (Fig 9(d)), can lead to formation of flux ropes [58], [59]. The formation of a flux rope by reconnection at a magnetic neutral line separating two polarities, based on a fully non-linear 3D MHD simulation, is illustrated in Fig. 10. Clearly the lower panel of this figure contains twisted fields whose projections have inverse-S shapes, just as Fig. 5 contains twisted fields whose projections have forward-S shapes.

### B. Topology

Once twisted magnetic fields are present on the spatial scales of observed sigmoids, there are two quite different possibilities for how they might be related to sigmoidal structures in X-rays. On the one hand, sigmoids may simply trace twisted fields within flux ropes, such as shown in Fig. 10, spheromak configurations [60], or linear force-free fields, such as Fig. 5. On the other hand, sigmoids may

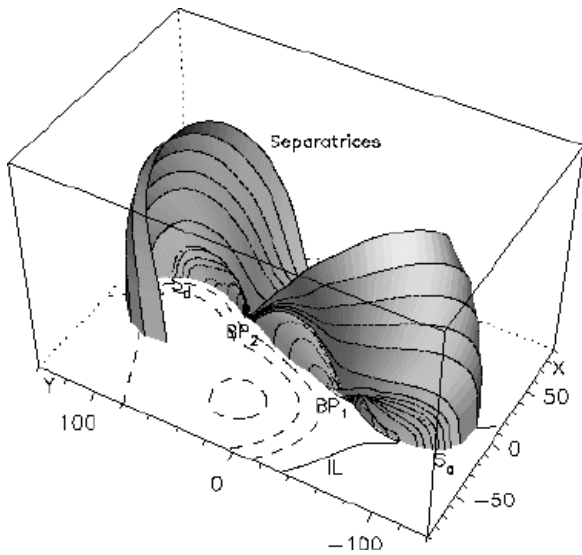


Fig. 11. A 3D view of the separatrices associated with a flux rope embedded in a surrounding potential magnetic field. The horizontal plane represents a photospheric magnetogram, showing contours of the magnetic flux density associated with the potential magnetic field and the magnetic polarity inversion line (IL). The points  $S_a$ ,  $BP_1$ ,  $BP_2$ , and  $S_d$  are elements of the topological skeleton. For esthetics the vertical height ( $z$ ) has been changed by the function  $30\sqrt{z}$ . By permission [56].

arise on only certain field lines which are special from a topological point of view.

Titov and Démoulin [56] consider sigmoids from a topological point of view. They developed approximate analytical expressions for the magnetic field that results when a force-free toroid, as shown in Figure 9(c), intrudes into a background potential field. The topological features of interest are the so-called separatrix surfaces, across which the magnetic field line connectivity suffers a jump. These are the sites at which magnetic reconnection can take place, allowing the conversion of magnetic energy into heat, mass motion, and enhanced X-ray emission. The manner in which the separatrices wrap around the twisted flux rope is shown in Figure 11. It is clear that X-ray emission from these surfaces will have a sigmoidal shape when viewed from above. In our opinion, this provides a very natural explanation for the sigmoids seen in the early phases of eruptive flares [28], when rapid magnetic reconnection might be expected along the separatrix. However, it is not clear that the sigmoidal patterns seen in the quiet corona and in steady-state structures of active regions are defined by such large-scale separatrix surfaces, as opposed to field lines within flux ropes (represented by the toroid in the Titov and Démoulin model).

### C. Eruption

Observers see ample evidence of helical structures in erupting solar filaments and CMEs [62]. However, there is no consensus among theorists on the physical mechanism by which such structures erupt – this is one of the major dueling grounds of solar physics. Some theorists argue that magnetic reconnection is of paramount importance,

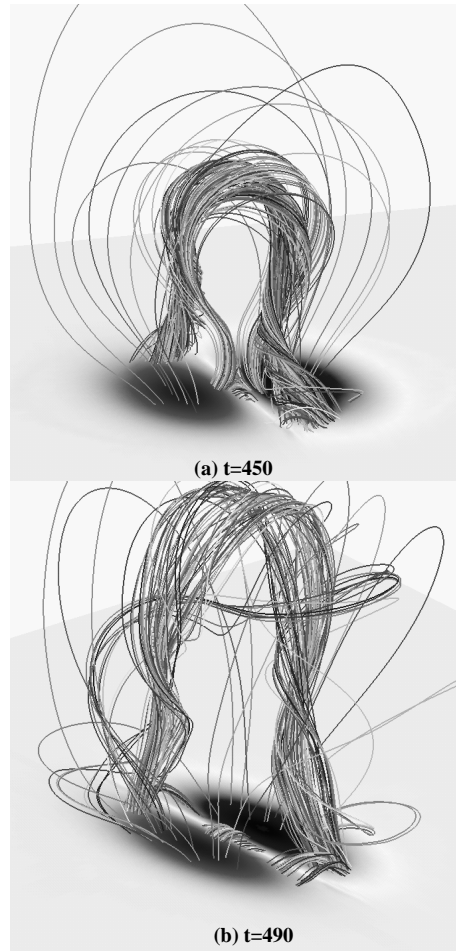


Fig. 12. Simulation of the eruption of magnetic fields during the relaxation of the configuration shown in Fig. 10 at  $t = 430\tau_A$ . By permission [61].

and we discuss that mechanism in this review. However, catastrophic loss of equilibrium, rather than magnetic reconnection, may be the primary mechanism driving eruption. Gravitational forces, at work on relatively massive filaments embedded in the otherwise magnetically dominated corona, may be important. These topics are discussed extensively in the solar physics literature [63], [64], [65], [66], [67], [68], [69], [70], [71], [72], [73]. We could not possibly do justice to the various issues, and will present only one example of recent work here.

Early theoretical work showed that simple bipolar force-free configurations twisted by more than  $\sim 2\pi$  steradians are linearly unstable [33], Sec. III-E. Nevertheless, there are various wrenches in the works [74], [75]. In virtually all magnetic configurations field line tying – the inhibition of transverse motions of magnetic field lines at their photospheric footpoints – has a stabilizing effect. As well, one

must do work to open up closed magnetic field lines such as all those shown in Fig. 9 [76], [77]. Hence, one may not necessarily expect an instability in a simple bipolar magnetic field to lead to a CME, unless one or more of the assumptions of the early models (no field lines that close within the corona, planar lower boundary condition) break down – as they do in many models currently being studied. Indeed, 3D ideal-MHD numerical simulations of the production of helical structures by shearing motions of fields in bipolar fields that are line-tied to a planar photosphere do not lead to eruption [75].

Continuing improvements in the physical realism of non-linear MHD simulations of the formation and eruption of 3D helical structures through shearing and diffusion in both planar geometry [59] and spherical geometry [78] encourage us to believe that solar physicists might someday understand the eruption of flux ropes. In the first phase of the planar simulations ( $0 < t < 400\tau_A$ , where  $\tau_A$  is the Alfvén time of the system) twisting and shearing, followed by viscous relaxation, drive reconnection near the magnetic polarity inversion line (Sec. IV-A) to form a sequence of twisted quasi-static structures (Fig. 10) reminiscent of the observations shown in Fig. 6. In the second phase ( $t > 400\tau_A$ ) new opposite-polarity flux is emerged, which changes the energetics [76], [77] appropriate to the work that must be done to open up the closed magnetic field structure. When the structures shown at  $t = 430\tau_A$  are subjected to such flux emergence, disruption takes place (Fig. 12) with liberation of a significant fraction of the stored magnetic energy.

## V. FUTURE WORK

It is straightforward to identify the areas in which work is required to make the discovery of a relationship between sigmoidal structures and proxies for white-light CMEs a useful tool for space weather forecasting:

- Improve the statistical basis for the link of white-light CMEs to proxies such as arcades, cusps, and transient coronal holes.
- Use measures of twist other than X-ray coronal morphology, i.e., photospheric vector magnetograms, chromospheric H-alpha images.
- Quantify the departure from potential structure by quantifying the degree of twist in the sigmoid [8].
- Take advantage of the sunspot area measurements to quantify the dependence of the eruption probability on this parameter.
- Develop an effective method for identifying sigmoids and their parameters in X-ray images, taking into account perspective effects.
- Extend the earlier study [31] to include sigmoids that are not in active regions.
- Extend the earlier study to flares.
- Incorporate time-to-eruption in the study.

## ACKNOWLEDGMENTS

The authors are pleased to acknowledge NASA’s support of this research under the Lockheed SXT contract NAS8-

40801 with Marshall Space Flight Center and MSU SR&T grant NAG5-6110. We thank T. Amari, P. Démoulin, and an anonymous referee for their comments.

## REFERENCES

- [1] S. Tsuneta, L. Acton, M. Bruner, J. Lemen, W. Brown, R. Carvalho, R. Catura, S. Freeland, B. Jurcevich, and J. Owens, “The soft x-ray telescope for the Solar-a mission,” *Solar Phys.*, vol. 136, pp. 37–67, Nov. 1991.
- [2] L. Acton, S. Tsuneta, Y. Ogawara, R. Bentley, M. Bruner, R. Canfield, L. Culhane, G. Doschek, E. Hiei, and T. Hirayama, “The Yohkoh mission for high-energy solar physics,” *Science*, vol. 258, pp. 618–625, Oct. 1992.
- [3] D. M. Rust and A. Kumar, “Helical magnetic fields in filaments,” *Solar Phys.*, vol. 155, pp. 69–97, Nov. 1994.
- [4] S. Kahler, “The morphological and statistical properties of solar x-ray events with long decay times,” *ApJ*, vol. 214, pp. 891–897, June 1977.
- [5] S. W. Kahler, “Solar flares and coronal mass ejections,” *ARA&A*, vol. 30, pp. 113–141, 1992.
- [6] D.F. Webb, “The origins, propagation and space weather aspects of coronal mass ejections,” *IEEE Transactions On Plasma Science, Special Issue on Space Plasmas*, 2000.
- [7] M. A. Berger, “Magnetic helicity in space physics,” in *Magnetic Helicity in Space and Laboratory Plasmas*, M. R. Brown, R. C. Canfield, and A. A. Pevtsov, Eds., Washington, D.C., 1999, vol. 111 of *Geophys. Monogr. Ser.*, pp. 1–10, AGU.
- [8] A. A. Pevtsov, R. C. Canfield, and A. N. McClymont, “On the subphotospheric origin of coronal electric currents,” *ApJ*, vol. 481, pp. 973–977, May 1997.
- [9] G. E. Brueckner, R. A. Howard, M. J. Koomen, C. M. Korndyke, D. J. Michels, J. D. Moses, D. G. Socker, K. P. Dere, P. L. Lamy, A. Llebaria, M. V. Bout, R. Schwenn, G. M. Simnett, D. K. Bedford, and C. J. Eyles, “The large angle spectroscopic coronagraph (LASCO),” *Solar Phys.*, vol. 162, pp. 357–402, 1995.
- [10] O. C. St. Cyr and 13 co authors, “Properties of coronal mass ejections: SOHO LASCO observations from January 1996 to June 1998,” *JGR*, p. submitted, 2000.
- [11] R. A. Howard, D. J. Michels, N. R. Sheeley, Jr., and M. J. Koomen, “The observation of a coronal transient directed at the Earth,” *ApJ*, vol. 263, pp. L101–L104, 1982.
- [12] D.F. Webb and E.W. Cliver, “Evidence for magnetic disconnection of mass ejections in the corona,” *JGR*, vol. 100, pp. 5,853–5,870, 1992.
- [13] G. M. Simnett and 18 co authors, “Lasco observations of disconnected magnetic structures out to beyond 28 solar radii during coronal mass ejections,” *Solar Physics*, vol. 175, pp. 685–698, Oct. 1997.
- [14] D.F. Webb, “The solar sources of coronal mass ejections,” in *IAU Colloq. 133: Eruptive Solar Flares*, 1992, pp. 234–247.
- [15] D. M. Rust, “Coronal disturbances and their terrestrial effects,” *Space Science Reviews*, vol. 34, pp. 21–36, 1983.
- [16] H. S. Hudson, “Yohkoh observations of coronal mass ejections,” in *Magnetodynamic phenomena in the solar atmosphere*, Y. Uchida, T. Kosugi, and H. S. Hudson, Eds. 1996, p. 89, Dordrecht: Kluwer Academic Publishers.
- [17] H. S. Hudson and D. F. Webb, “Soft x-ray signatures of coronal ejections,” in *Coronal Mass Ejections: Causes and Consequences*, N. Crooker, J. Joselyn, and J. Feynman, Eds., Washington, D.C., 1997, vol. 99 of *Geophys. Monogr. Ser.*, pp. 27–37, AGU.
- [18] J. I. Khan and H. S. Hudson, “Homologous sudden disappearances of transequatorial loops in the solar corona,” *Geophys. Res. Lett.*, vol. submitted, 2000.
- [19] H. S. Hudson et al., “Yohkoh/SXT soft x-ray observations of sudden mass loss from the solar corona,” in *Solar Wind Eight*, D. Winterhalter, J. T. Gosling, S. R. Habbal, W. S. Kurth, and M. Neugebauer, Eds., 1995, vol. 382 of *AIP Conference Proceedings*, pp. 88–91.
- [20] H. S. Hudson, L. W. Acton, and S. F. Freeland, “A long-duration solar flare with mass ejection and global consequences,” *ApJ*, vol. 470, pp. 629–635, 1996.
- [21] J. P. Wild, S. F. Smerd, and A. A. Weiss, “Solar bursts,” *ARA&A*, vol. 1, pp. 291, 1963.
- [22] R. G. Athay and G. E. Moreton, “Impulsive phenomena of the



- solar atmosphere. I. Some optical events associated with flares showing explosive phase," *ApJ*, vol. 133, pp. 935, 1961.
- [23] Y. Uchida, "Propagation of hydromagnetic disturbances in the solar corona and Moreton's phenomenon," *Solar Phys.*, vol. 4, pp. 30, May 1968.
- [24] N. Gopalswamy, M. L. Kaiser, R. P. Lepping, S. W. Kahler, K. Ogilvie, D. Berdichevsky, T. Kondo, T. Isobe, and M. Akioka, "Origin of coronal and interplanetary shocks - a new look with Wind spacecraft data," *JGR*, vol. 103, pp. 307, 1998.
- [25] B. J. Thompson, J. B. Gurman, W. M. Neupert, J. S. Newmark, J.-P. Delaboudinière, O. C. St. Cyr, S. Stezelberger, K. P. Dere, Howard, R. A., and D. J. Michels, "SOHO/EIT observations of the 1997 April 7 coronal transient: Possible evidence of coronal moreton waves," *ApJ*, vol. 517, pp. L151-L154, 1999.
- [26] H. S. Hudson, J. I. Khan, J. R. Lemen, B. J. Thompson, and Y. Uchida, "Soft x-ray observation of a large-scale coronal wave and its exciter," *ApJ*, vol. submitted, 2000.
- [27] T. Sakurai, K. Shibata, K. Ichimoto, S. Tsuneta, and L. W. Acton, "Flare-related relaxation of magnetic shear as observed with the soft x-ray telescope of Yohkoh and with vector magnetographs," *pasj*, vol. 44, pp. L123-L127, Oct. 1992.
- [28] D. M. Rust and A. Kumar, "Evidence for helically kinked magnetic flux ropes in solar eruptions," *ApJ*, vol. 464, pp. L199-L202, June 1996.
- [29] A. C. Sterling and H. S. Hudson, "Yohkoh SXT observations of x-ray "dimming" associated with a halo coronal mass ejection," *ApJ*, vol. 491, pp. L55-L58, Dec. 1997.
- [30] H. S. Hudson, J. R. Lemen, O. C. St. Cyr, A. C. Sterling, and D. F. Webb, "X-ray coronal changes during halo CMEs," *Geophys. Res. Lett.*, vol. 25, pp. 2481-2484, 1998.
- [31] R. C. Canfield, H. S. Hudson, and D. E. McKenzie, "Sigmoidal morphology and eruptive solar activity," *Geophys. Res. Lett.*, vol. 26, pp. 627, Mar. 1999.
- [32] R. G. Giovanelli, "The relations between eruptions and sunspots," *ApJ*, vol. 89, pp. 555-567, June 1939.
- [33] E. R. Priest, "Solar magneto-hydrodynamics," in *Geophysics and Astrophysics Monographs, Dordrecht: Reidel, 1984*, 1984.
- [34] A. A. Pevtsov, R. C. Canfield, and T. R. Metcalf, "Latitudinal variation of helicity of photospheric magnetic fields," *ApJ*, vol. 440, pp. L109-L112, Feb. 1995.
- [35] A. A. van Ballegoijen, "Photospheric motions as a source of twist in the photosphere and corona," in *Magnetic Helicity in Space and Laboratory Plasmas*, M. R. Brown, R. C. Canfield, and A. A. Pevtsov, Eds., Washington, D.C., 1999, vol. 111 of *Geophys. Monogr. Ser.*, pp. 213-220, AGU.
- [36] K. D. Leka, R. C. Canfield, A. N. McClymont, and L. van Driel-Gesztelyi, "Evidence for current-carrying emerging flux," *ApJ*, vol. 462, pp. 547, May 1996.
- [37] R. C. Canfield and A. A. Pevtsov, "Helicity and reconnection in the solar corona: Observations," in *Magnetic Helicity in Space and Laboratory Plasmas*, M. R. Brown, R. C. Canfield, and A. A. Pevtsov, Eds., Washington, D.C., 1999, vol. 111 of *Geophys. Monogr. Ser.*, pp. 197-204, AGU.
- [38] A. A. Pevtsov and R. C. Canfield, "Helicity of the photospheric magnetic field," in *Magnetic Helicity in Space and Laboratory Plasmas*, M. R. Brown, R. C. Canfield, and A. A. Pevtsov, Eds., Washington, D.C., 1999, vol. 111 of *Geophys. Monogr. Ser.*, pp. 103-110, AGU.
- [39] D. W. Longcope, M.G. Linton, A. A. Pevtsov, G. H. Fisher, and I. Klapper, "Twisted flux tubes and how they get that way," in *Magnetic Helicity in Space and Laboratory Plasmas*, M. R. Brown, R. C. Canfield, and A. A. Pevtsov, Eds., Washington, D.C., 1999, vol. 111 of *Geophys. Monogr. Ser.*, pp. 93-101, AGU.
- [40] V. Bothmer and D. M. Rust, "The field configuration of magnetic clouds and the solar cycle," in *Coronal Mass Ejections*, N. Crooker, J. Joselyn, and J. Feynman, Eds., Washington, D.C., 1997, vol. 99 of *Geophys. Monogr. Ser.*, pp. 139-146, AGU.
- [41] A. A. Pevtsov, R. C. Canfield, and H. Zirin, "Reconnection and helicity in a solar flare," *ApJ*, vol. 473, pp. 533-538, Dec. 1996.
- [42] J. T. Gosling, "The role of reconnection in the formation of flux ropes in the solar wind," in *Magnetic Helicity in Space and Laboratory Plasmas*, M. R. Brown, R. C. Canfield, and A. A. Pevtsov, Eds., Washington, D.C., 1999, vol. 111 of *Geophys. Monogr. Ser.*, pp. 205-212, AGU.
- [43] D. F. Webb, E. W. Cliver, N. U. Crooker, O. C. St. Cyr, and B. J. Thompson, "The relationship of halo CMEs, magnetic clouds and magnetic storms," *JGR*, p. in press, 2000.
- [44] R. C. Canfield and K. P. Reardon, "The eruptive flare of 15 november 1991: Preflare phenomena," *Solar Phys.*, vol. 182, pp. 145-157, Sept. 1998.
- [45] H. Ji, S. C. Prager, and J. S. Sarff, "Conservation of magnetic helicity during plasma relaxation," *Phys. Rev. Lett.*, vol. 74, no. 15, pp. 2945-2948, apr 1995.
- [46] R. C. Canfield, A. A. Pevtsov, and A. N. McClymont, "Magnetic chirality and coronal reconnection," in *Magnetic Reconnection in the Solar Atmosphere*, R. D. Bentley and J. T. Mariska, Eds. 1996, vol. 111 of *Conf. Ser.*, pp. 341-346, Astron. Soc. of the Pacific.
- [47] D. B. Melrose, "A solar flare model based on magnetic reconnection between current-carrying loops," *ApJ*, vol. 486, pp. 521-533, Sept. 1997.
- [48] R. C. Chase, A. S. Krieger, Z. Svestka, and G. S. Vaiana, "Skylab observations of x-ray loops connecting separate active regions," in *Space Research*, M. J. Rycroft, Ed., Berlin, 1976, vol. XVI, pp. 917-922, Akademie-Verlag.
- [49] Z. Svestka, A. S. Krieger, R. C. Chase, and R. Howard, "Transequatorial loops interconnecting McMath regions 12472 and 12474," *Solar Phys.*, vol. 52, pp. 69-90, Apr. 1977.
- [50] S. Tsuneta, "Interacting active regions in the solar corona," *ApJ*, vol. 456, pp. L63-L65, Jan. 1996.
- [51] F. Farnik, M. Karlicky, and Z. Svestka, "Long transequatorial interconnecting loops of the new solar cycle," *Solar Phys.*, vol. 187, pp. 33-44, June 1999.
- [52] J. Feynman, "Evolving magnetic structures and their relation to coronal mass ejections," in *Coronal Mass Ejections*, N. Crooker, J. A. Joselyn, and J. Feynman, Eds., Washington, D.C., 1997, *Geophys. Monogr. Ser.*, pp. 49-55, AGU.
- [53] R. C. Canfield and A. A. Pevtsov, "Helicity of solar active region magnetic fields," in *Synoptic Solar Physics*, K. S. Balasubramanian, J. W. Harvey, and D. M. Rabin, Eds. 1997, pp. 131-143, A. S. P.
- [54] H. Zhang and S. Bao, 1998, private communication.
- [55] E. R. Priest, "Magnetic helicity and relaxation phenomena in the solar corona," in *Magnetic Helicity in Space and Laboratory Plasmas*, M. R. Brown, R. C. Canfield, and A. A. Pevtsov, Eds., Washington, D.C., 1999, vol. 111 of *Geophys. Monogr. Ser.*, pp. 141-148, AGU.
- [56] V. S. Titov and P. Démoulin, "Basic topology of twisted magnetic configurations in solar flares," *A&A*, vol. 351, pp. 707-720, Nov. 1999.
- [57] P. A. Gilman and P. Charbonneau, "Creation of twist at the core-convection zone interface," in *Magnetic Helicity in Space and Laboratory Plasmas*, M. R. Brown, R. C. Canfield, and A. A. Pevtsov, Eds., Washington, D.C., 1999, vol. 111, pp. 75-82, AGU.
- [58] A. A. van Ballegoijen and P. C. H. Martens, "Formation and eruption of solar prominences," *ApJ*, vol. 343, pp. 971-984, Aug. 1989.
- [59] T. Amari and J. F. Luciani, "Confined disruption of a three-dimensional twisted magnetic flux tube," *ApJ*, vol. 515, pp. L81-L84, Apr. 1999.
- [60] S. E. Gibson and B. C. Low, "3-D and twisted: An MHD interpretation of on-disk observational characteristics of CMEs," *JGR*, vol. in press, 2000.
- [61] T. Amari, J. F. Luciani, Z. Mikic, and J. Linker, "A twisted flux rope model for coronal mass ejections and two ribbon flares," *ApJ*, vol. submitted, 2000.
- [62] D. M. Rust, "Magnetic helicity in solar filaments and coronal mass ejections," in *Magnetic Helicity in Space and Laboratory Plasmas*, M. R. Brown, R. C. Canfield, and A. A. Pevtsov, Eds., Washington, D.C., 1999, vol. 111 of *Geophys. Monogr. Ser.*, pp. 221-228, AGU.
- [63] J. Birn and K. Schindler, "Two-ribbon flares: Magnetostatic equilibria," in *Solar Flare Magnetohydrodynamics*, E. R. Priest, Ed., New York, 1981, vol. 1 of *The Fluid Mechanics of Astrophysics and Geophysics*, pp. 337-377, Gordon and Breach Science Publishers.
- [64] R. L. Moore, "Evidence that magnetic energy shedding in solar filament eruptions is the drive in accompanying flares and coronal mass ejections," *ApJ*, vol. 324, pp. 1132-1137, Jan. 1988.
- [65] T. G. Forbes, "Numerical simulation of a catastrophe model for coronal mass ejections," *JGR*, vol. 95, pp. 11919-11931, Aug. 1990.
- [66] B. C. Low, "Equilibrium and dynamics of coronal magnetic fields," *ARA&A*, vol. 28, pp. 491-524, 1990.

- [67] T. G. Forbes and P. A. Isenberg, "A catastrophe mechanism for coronal mass ejections," *ApJ*, vol. 373, pp. 294–307, May 1991.
- [68] T. G. Forbes, "Magnetic reconnection in solar flares," *Geophys. Astrophys. Fluid Dyn.*, vol. 62, pp. 16–36, 1991.
- [69] R. Wolfson and B. C. Low, "Energy buildup in sheared force-free magnetic fields," *ApJ*, vol. 391, pp. 353–358, May 1992.
- [70] P. A. Isenberg, T. G. Forbes, and P. Demoulin, "Catastrophic evolution of a force-free flux rope: A model for eruptive flares," *ApJ*, vol. 417, pp. 368–386, Nov. 1993.
- [71] T. G. Forbes and E. R. Priest, "Photospheric magnetic field evolution and eruptive flares," *ApJ*, vol. 446, pp. 377–389, June 1995.
- [72] B. C. Low, "Solar activity and the corona," *Solar Phys.*, vol. 167, pp. 217–265, Aug. 1996.
- [73] J. Lin, T. G. Forbes, P. A. Isenberg, and P. Demoulin, "The effect of curvature on flux-rope models of coronal mass ejections," *ApJ*, vol. 504, pp. 1006–1019, Sept. 1998.
- [74] J. A. Klimchuk and P. A. Sturrock, "Force-free magnetic fields - is there a 'loss of equilibrium'?", *ApJ*, vol. 345, pp. 1034–1041, Oct. 1989.
- [75] S. K. Antiochos, "The role of helicity in magnetic reconnection: 3d numerical simulations," in *Magnetic Helicity in Space and Laboratory Plasmas*, M. R. Brown, R. C. Canfield, and A. A. Pevtsov, Eds., Washington, D.C., 1999, vol. 111 of *Geophys. Monogr. Ser.*, pp. 187–196, AGU.
- [76] J. J. Aly, "How much energy can be stored in a three-dimensional force-free magnetic field?," *ApJ*, vol. 375, pp. L61–L64, July 1991.
- [77] P. A. Sturrock, "Maximum energy of semi-infinite magnetic field configurations," *ApJ*, vol. 380, pp. 655–659, Oct. 1991.
- [78] Z. Mikic and J. A. Linker, "Initiation of coronal mass ejections by changes in photospheric flux," in *American Astronomical Society Meeting*, May 1999, vol. 194, pp. 5906+.